

# Inference for Model Misspecification in Interest Rate Term Structure using Functional Principal Component Analysis

Kaiwen Hou\*

December 22, 2022

## Abstract

Level, slope, and curvature are three commonly-believed principal components in interest rate term structure and are thus widely used in modeling. This paper characterizes the heterogeneity of how misspecified such models are through time. Presenting the orthonormal basis in the Nelson-Siegel model interpretable as the three factors, we design two nonparametric tests for whether the basis is equivalent to the data-driven functional principal component basis underlying the yield curve dynamics, considering the ordering of eigenfunctions or not, respectively. Eventually, we discover high dispersion between the two bases when rare events occur, suggesting occasional misspecification even if the model is overall expressive.

**Keywords:** Interest Rate, Term Structure, Model Misspecification, Principal Component Analysis, Functional Data Analysis

**JEL Codes:** C14, C38, C44, C52

---

\*Columbia Business School, kaiwen.hou@columbia.edu

# 1 Introduction

The dynamic evolution of the interest rate term structure is indispensable for many tasks, including pricing interest rate derivatives, discounting future payoff for asset prices, explaining return predictability, conducting firm evaluations, managing financial risk, making monetary and fiscal policy (Elenev et al., 2021; Elenev, Landvoigt and Van Nieuwerburgh, 2022; Krishnamurthy and Vissing-Jorgensen, 2011; Woodford, 2012), and most importantly, forecasting rare events like financial crises and predicting future growth Hu, Pan and Wang (2013); Kojien, Lustig and Van Nieuwerburgh (2017).

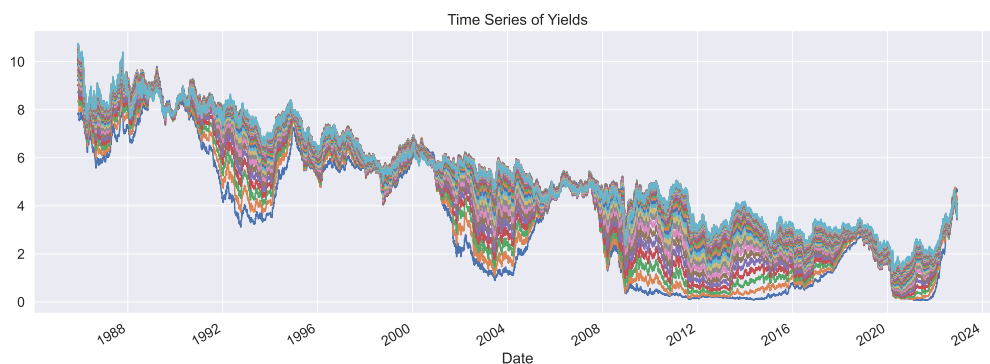


Figure 1: Time series of zero-coupon yields on different bond maturities shows heteroscedastic covariation of yield curves.

There *seems* to be a linear structure in the interest rate term structure *most of the times*. Eigendecomposition of the covariance matrix of yield changes attributes over 97% of the variance to three principal components, known as the level, the slope, and the curvature, seemingly universal across different units of maturity (Chapman and Pearson, 2001; Litterman and Scheinkman, 1991; Piazzesi, 2010). Using the daily zero-coupon yield curve of bonds maturing in 1 year to 30 years (Gürkaynak, Sack and Wright, 2007) from November 25, 1985<sup>1</sup>, to December 9, 2022, we obtain the first three principal components of the entire dataset in Figure 2.

---

<sup>1</sup>The data starts in 1985 after dropping the missing and incomplete data, so that all cross-sectional data points have observations from hypothetical securities with 1-year to 30-year maturity. The missing data before was mainly due to lack of actual securities for model calibration.

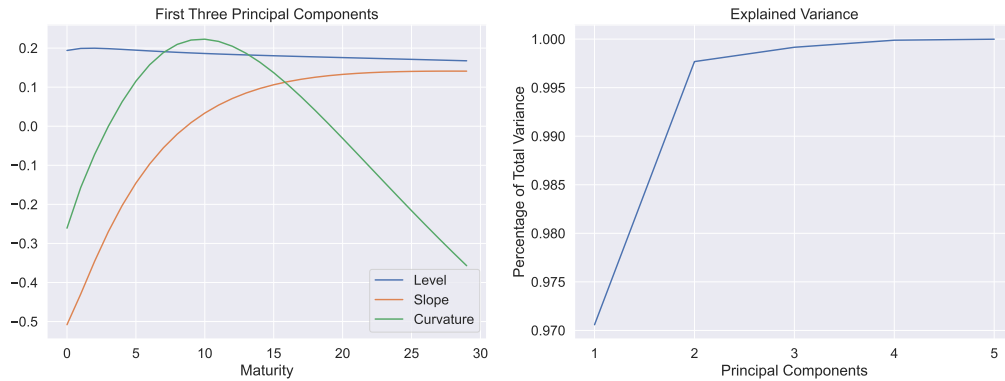


Figure 2: First three principal components of the entire dataset and explained variance ratios.

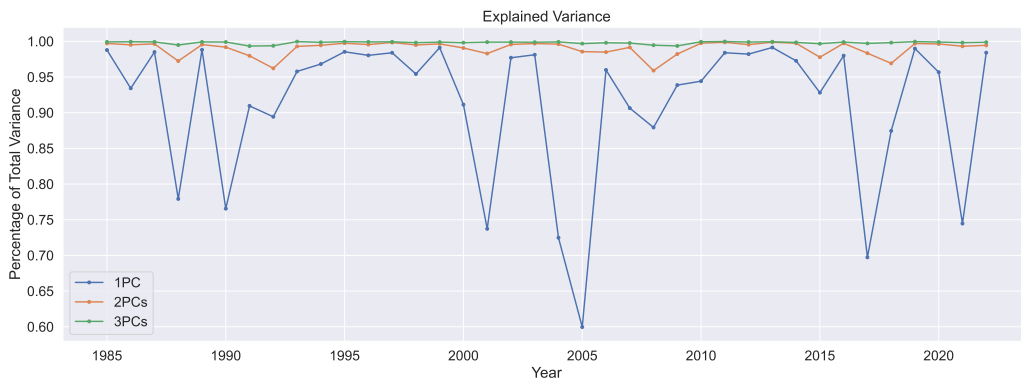


Figure 3: Explained variance by first 1/2/3 principal components in each year.

On the other hand, a dispersion in actual yields around the smooth term structure has been used to measure liquidity, whose friction spikes in crises while remaining small otherwise (Hu, Pan and Wang, 2013). Following Fama and MacBeth (1973) regression and construction of a factor mimicking portfolio (Ang et al., 2006), a significant liquidity premium is revealed so that the noise measure passes the cross-sectional test. However, the decent returns gained from trading illiquidity do not necessarily suggest that the interest-rate model is well-specified, nor does it justify using a smooth three-factor term structure model as a reference model (as in Hu, Pan and Wang (2013)) from which dispersion is measured.

To put it in another way, even if the first three principal components can explain a high variance in the yield curves (which also means that reconstruction error is low), as

shown in Figure 3, and even if the full-sample stylistic features (in Figure 2) of first three principal components have an immaculate interpretation of their shapes, the three principal components do not always correspond to the level, slope, and curvature factors from a more granular perspective - in some years they may not have rich economic interpretations at all (Lord and Pelsser, 2007). Indeed, from Figure 4, the level-slope-curvature seems to be occasionally violated, as sometimes the first principal component (which “ought to be” the level) is not flat (e.g., in 2007 and 2017), and the second principal component (which “ought to be” the slope) is not monotonic (e.g., in 1990, 2008, and 2021).

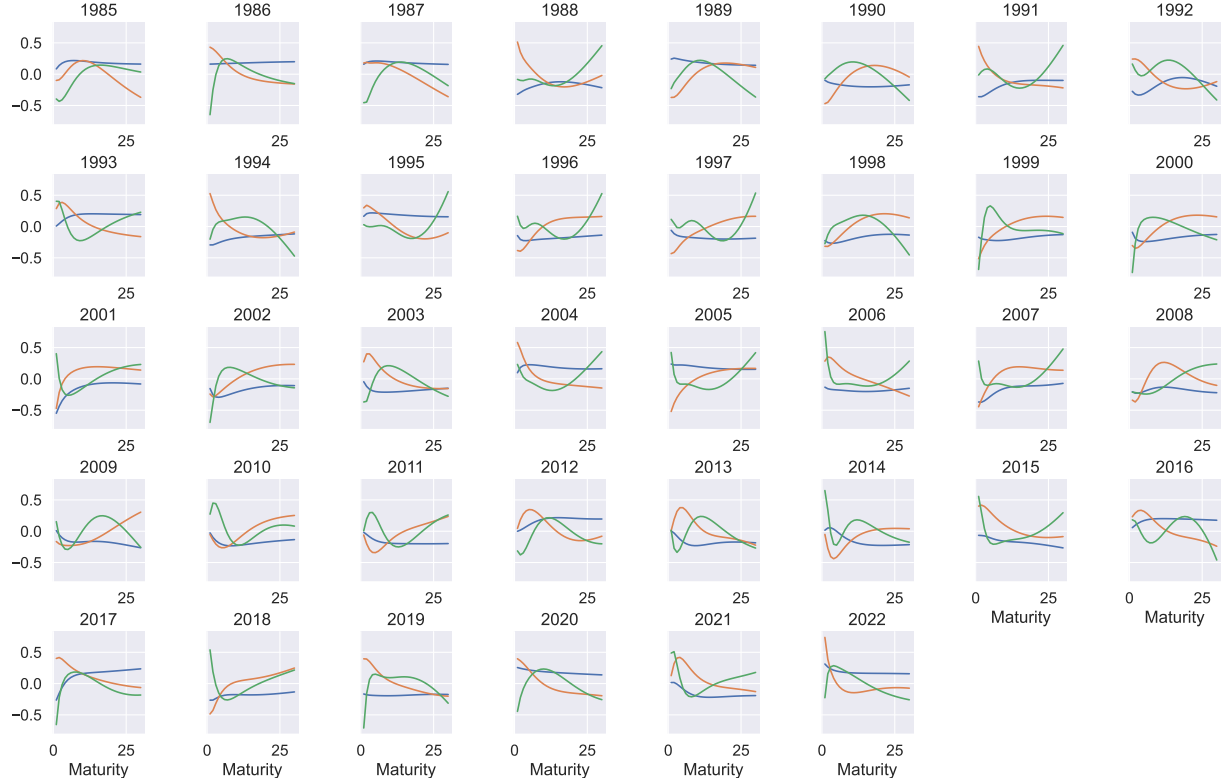


Figure 4: Loadings of first three principal components in each year. Blue curves represent the first principal component or the “level” factor; orange curves represent the second principal component or the “slope” factor; green ones represent the third principal component or the “curvature”.

With such economic interpretations being invalidated occasionally, some standard models of interest rate term structure based on these interpretations, such as Nelson and Siegel (1987), might problematically impose a specific smooth structure of yield curves, and the

dispersion from a smooth yield curve that Hu, Pan and Wang (2013) benchmarks against could be a biased benchmark.

As pointed out in previous literature, model misspecification (also known as model uncertainty or ambiguity) should be acknowledged in macroeconomic theory (Hansen and Sargent, 2001*a,b*); market participants probably have a preference towards robustness (Anderson, Hansen and Sargent, 2000; Hansen, Sargent and Tallarini Jr, 1999; Maenhout, 2004); the monetary policies could have differed a lot when the actual model describing the environment appears ambiguous to the central bank (Giannoni, 2002; Hansen and Sargent, 2010; Kasa, 2002; Onatski and Stock, 2002; Woodford, 2010). It is also likely that interest rate models also suffer from misspecification (Brenner, Harjes and Kroner, 1996), mainly when market crashes or jumps are observed in continuous time (Johannes, 2004). Despite the overall satisfactory exponentially affine term structure models, the moments of latent variables present in the affine structure could also be ambiguous (Liu, Wang and Zhang, 2018; Liu et al., 2022; Zhang, Cheng and Wang, 2022), leading to a misspecified affine model.

In light of Hu, Pan and Wang (2013), this paper examines the model misspecification of interest rate term structures both on an omniscient scope and a granular perspective. Figure 5 presents the functional data structure we have, i.e., the time series of term structure as a function, which motivates our methodology different from the inadequate conventional one. We utilize recent advances in functional data analysis, particularly a nonparametric hypothesis test of functional principal component analysis (FPCA), and compare its results implied by classical principal component analysis (PCA), which highly relies on the homogeneity of term structure throughout time. Instead of directly constructing a stochastic partial differential equation to model the interest rate dynamics as a stochastic process in the space of functions (Cont, 2005), we employ the nonparametric and distribution-free method in this research to lean on minimal assumptions.

Our codes are released on <https://github.com/Kaiwen-Hou-KHou/termStructureFPCA>.

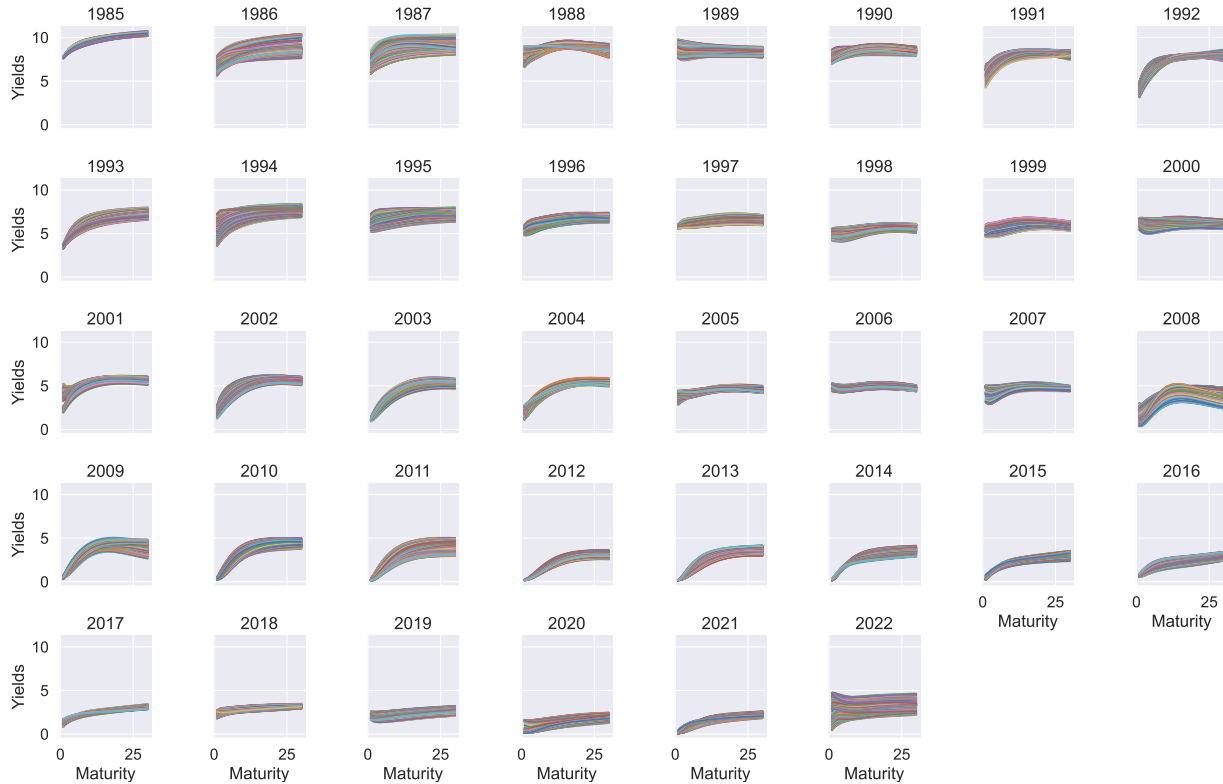


Figure 5: Daily yield curves from 1985 to 2022.

## 2 Preliminaries

In this section, we introduce the essential statistical and econometric tools to deal with functional data such as the time series of yield curves, including a generalization of classical principal component analysis and eigendecomposition into infinite-dimension space  $L^2([0, 1], d\xi)$  (the space of square-integrable functions on  $[0, 1]$ , where the inner product weighted by the constant function 1 is defined as  $\langle f, g \rangle := \int_0^1 fg d\xi$ ), the assumption of smoothness and smoothing techniques, followed by some asymptotics that helps examine FPCA method through statistical inference.

## 2.1 Functional Principal Component Analysis

A generalized PCA method, FPCA is developed to investigate the dominant modes of functional data variation, such as modeling sparse longitudinal data or conducting functional classification and regression (Hall, Müller and Wang, 2006; Li and Hsing, 2010; Yao, Müller and Wang, 2005*a,b*).

Let  $y_i$  be i.i.d. samples of a random function  $y : (\Omega, \mathcal{F}, P) \rightarrow (C^0[0, 1], \mathcal{B}_{C[0,1]})$  with  $\mathbb{E}\|y\|^2 < \infty$ . Denote by

$$m = \mathbb{E}y \in L^2([0, 1], d\xi)$$

the mean function, and by

$$G(x, x') = Cov(y(x), y(x')) \in L^2([0, 1]^2, d\xi d\xi')$$

the covariance function<sup>2</sup>. By Mercer's theorem, there exists a sequence of eigenvalues  $\lambda_k \downarrow 0$  such that  $\sum_{k=1}^{\infty} \lambda_k < \infty$  and

$$G(x, x') = \sum_{k=1}^{\infty} \lambda_k \psi_k(x) \psi_k(x'),$$

where the orthonormal basis functions  $(\psi_k)_{k=1}^{\infty}$  are the eigenfunctions satisfying

$$\int_0^1 G(x, x') \psi_k(x') dx' = \lambda_k \psi_k(x).$$

By the Kosambi–Karhunen–Loève theorem (Kosambi, 2016), one can write

$$\xi_i = y_i - m = \sum_{k=1}^{\infty} \zeta_{ik} \psi_k,$$

where the principal component<sup>3</sup> associated with the  $k$ -th eigenfunction  $\psi_k$  is  $\zeta_{ik} = \langle \xi_i, \psi_k \rangle$

---

<sup>2</sup>Since covariance is symmetric (and continuous here), then  $G$  is a positive semi-definite kernel, so Mercer's theorem applies.

<sup>3</sup> $\zeta_{ik}$  is also known as the rescaled functional principal component scores.

with the following moment properties

$$\begin{aligned}\mathbb{E}\zeta_{ik} &= 0, \\ \mathbb{E}\zeta_{ik}^2 &= \lambda_k, \\ \mathbb{E}\zeta_{ik}\zeta_{ik'} &= 0,\end{aligned}$$

for all  $1 \leq i \leq n$ , and  $k \neq k' \in \mathbb{N}^+$ .

It is also justified in Cont (2005) and Kusuoka (2000)<sup>4</sup> that the term structure could be modeled to have a two-dimensional dynamics (time and maturity), even if the dynamics on maturity is slightly anti-intuitive. Therefore, the interest rate term structure fits in this stochastic framework.

## 2.2 Smoothness

Note that a crucial assumption of FPCA is that data are modeled as sample paths of smooth stochastic processes, although they are often observed discretely and noisily. If sample paths are not smooth, then  $G \notin L^2([0, 1]^2, d\xi d\xi')$ . Fortunately, this assumption can be relaxed by restricting  $G$  to a subset to model some diffusion processes. For example, standard Brownian motion has non-differentiable covariance  $G(x, x') = \min(x, x')$  on the diagonal, but it becomes  $G(x, x') = x$ , which is infinitely differentiable when restricted on the upper-triangular block

$$\text{UT} := \{(x, x') \mid 0 \leq x < x' \leq 1\}. \quad (1)$$

With similar restriction, the covariance functions of common diffusion processes such as Brownian bridge, geometric Brownian motion, and Ornstein-Uhlenbeck process (Jouzdani and Panaretos, 2021) would also lie in  $L^2([0, 1]^2, d\xi d\xi')$ .

For discrete observations, methods like local linear or spline smoothing can be used to obtain the functional form of *each*  $y_i$  (Yao, Müller and Wang, 2005a). In particular, if

---

<sup>4</sup>This is a work suggested by Professor Darrell Duffie.

observations are evenly-spaced at  $\left(\frac{j}{N}\right)_{j=1}^N$ , one can adopt the B-spline estimator by projecting the discrete-valued function  $y_i$  to the space  $\mathcal{H}^{(p-2)}[0, 1]$  spanned by B-splines of order  $p$ :

$$\hat{y}_i = \arg \min_{g \in \mathcal{H}^{(p-2)}[0,1]} \sum_{j=1}^N \left\{ y_i \left( \frac{j}{N} \right) - g \left( \frac{j}{N} \right) \right\}^2. \quad (2)$$

Correspondingly, the smoothed and centered process is estimated by

$$\hat{\xi}_i = \hat{y}_i - \hat{m} = \hat{y}_i - \frac{1}{n} \sum_{j=1}^n \hat{y}_j.$$

Getting rid of the diagonal components in  $G$  by restrictions in Eq. (1) also ignores the measurement errors after smoothing (Staniswalis and Lee, 1998).

In dealing with interest rate term structures, their smoothness has been a reasonable assumption as widely used in interpolating yield curves, which rely on piecewise smooth functions that are also smoothly joined at selected knots Christensen, Diebold and Rudebusch (2011); Diebold and Li (2006); Diebold, Li and Yue (2008); Fisher, Nychka and Zervos (1995); McCulloch (1975); Nelson and Siegel (1987); Svensson (1994).

## 2.3 Hypothesis Testing

Given an orthonormal set  $(\psi_{0k})_{k=1}^\infty$ , Song, Yang and Zhang (2022) propose a statistical test for the hypothesis  $H_0$  that the eigenfunctions  $(\psi_k)_{k=1}^\infty$  form the same set up to permutations and change of signs. Fixing a hyper-parameter  $\kappa_n$ , the test statistic is

$$\hat{S}_n = n \sum_{1 \leq k < k' \leq \kappa_n} \hat{Z}_{kk'}^2, \quad (3)$$

where

$$\hat{Z}_{kk'} = \left\langle \hat{G}(x, x'), \psi_{0k}(x) \psi_{0k'}(x') \right\rangle_{L^2([0,1]^2, d\xi d\xi')} := \int_0^1 \int_0^1 \hat{G}(x, x') \psi_{0k}(x) \psi_{0k'}(x') dx dx',$$

with the two-step estimate of the covariance

$$\hat{G}(x, x') = \frac{1}{n} \sum_{i=1}^n \hat{\xi}_i(x) \hat{\xi}_i(x'). \quad (4)$$

Note that  $\hat{G}$  is essentially a low-rank approximation of the bi-infinite covariance matrix, as  $y_i$  has been projected onto  $\mathcal{H}^{(p-2)}[0, 1]$ . This naïve sub-block estimator is genuinely a choice out of simplicity; one could also adopt stochastic estimation such as the Russian roulette estimator to attain unbiasedness (Hou and Rabusseau, 2022).

It has also been shown in Song, Yang and Zhang (2022) that the asymptotic distribution of the test statistic under  $H_0$  is an infinite Gaussian quadratic form, and a finite sample estimator of its quantile  $\hat{Q}_{1-\alpha}$ , which is the  $100(1 - \alpha)$ -th percentile of

$$\bar{S}_n = \sum_{1 \leq k < k' \leq \kappa_n} \hat{\lambda}_k \hat{\lambda}_{k'} \chi_{kk'}^2(1), \quad (5)$$

is consistent. Here

$$\hat{\lambda}_k = \frac{1}{n} \sum_{i=1}^n \hat{\zeta}_{ik}^2,$$

where

$$\hat{\zeta}_{ik} = \left\langle \hat{\xi}_i, \psi_{0k} \right\rangle.$$

The distribution of the Gaussian quadratic form  $\bar{S}_n$  in Eq. (5) is essentially a weighted sum of  $\chi^2(1)$  random functions, where the weights are the eigenvalue pairs of  $G$ . In the special case where these eigenvalues are 1, the distribution becomes  $\chi^2\left(\frac{\kappa_n(\kappa_n-1)}{2}\right)$ , but this does not hold in general, as the scale parameter of a gamma distribution changes when multiplied by a constant and  $\hat{\lambda}_k \hat{\lambda}_{k'} \chi_{kk'}^2(1)$  might be no longer of Chi-squared distribution. Unfortunately,  $\bar{S}_n$  does not have a neat closed-form representation of its density or distribution function, so its quantiles should probably be computed numerically (Bodenham and Adams, 2016; Davies, 1980).

### 3 Nelson-Siegel Model

The Nelson-Siegel model (Nelson and Siegel, 1987) fits the yield curve with a simple functional form

$$\hat{y}(\tau | \Theta) = \beta_0 + \beta_1 \frac{1 - e^{-\theta\tau}}{\theta\tau} + \beta_2 \left( \frac{1 - e^{-\theta\tau}}{\theta\tau} - e^{-\theta\tau} \right), \quad (6)$$

where the parameters are  $\Theta = (\beta_0, \beta_1, \beta_2, \theta)$  and  $\tau$  is the maturity in months<sup>5</sup>.

It is acknowledged (e.g., by Diebold and Li (2006); Diebold, Li and Yue (2008)) that  $\beta_0, \beta_1$ , and  $\beta_2$  represent loadings on the level factor, the slope factor, and the curvature factor, respectively, so Eq. (6) can be generalized to the dynamic Nelson-Siegel Model in the following Eq. (7)

$$\hat{y}_t(\tau | \Theta) = L_t + S_t \frac{1 - e^{-\theta\tau}}{\theta\tau} + C_t \left( \frac{1 - e^{-\theta\tau}}{\theta\tau} - e^{-\theta\tau} \right), \quad (7)$$

through adding the auto-regressive state variables  $L_t$  for level,  $S_t$  for slope, and  $C_t$  for curvature.

We now proceed to test whether the orthonormal basis beneath the three factors  $1, \frac{1 - e^{-\theta\tau}}{\theta\tau}$  and  $\left( \frac{1 - e^{-\theta\tau}}{\theta\tau} - e^{-\theta\tau} \right)$  is equivalent to the actual principal component basis to see if the level, slope, and curvature factors always explain the major variation in the interest rate term structures, and offer insights on the dispersion between the two bases.

#### 3.1 Orthonormalization

Typically the tradable bond maturity in months is bounded both from above and from below, i.e.,  $0 < \underline{\tau} \leq \tau \leq \bar{\tau}$ . We can reproduce Eq. (6) in the following theorem so that  $\tau$  is rescaled in  $[0, 1]$ .

**Theorem 1.** *There exist three orthonormal basis functions  $\psi_{0k} \in L^2([0, 1], d\xi)$  ( $k = 1, 2, 3$ ) such that the Nelson-Siegel term structure  $\hat{y} \in \text{Span}(\psi_{0k})_{k=1}^3 \subset L^2([0, 1], d\xi)$ .*

---

<sup>5</sup>The model is invariant with respect to the unit of maturity, as  $\theta$  absorbs the scale difference between units. For example, transforming  $\tilde{\theta} = 12\theta$  and  $\tilde{\tau} = \frac{\tau}{12}$  in years, Eq. (6) is of the same form.

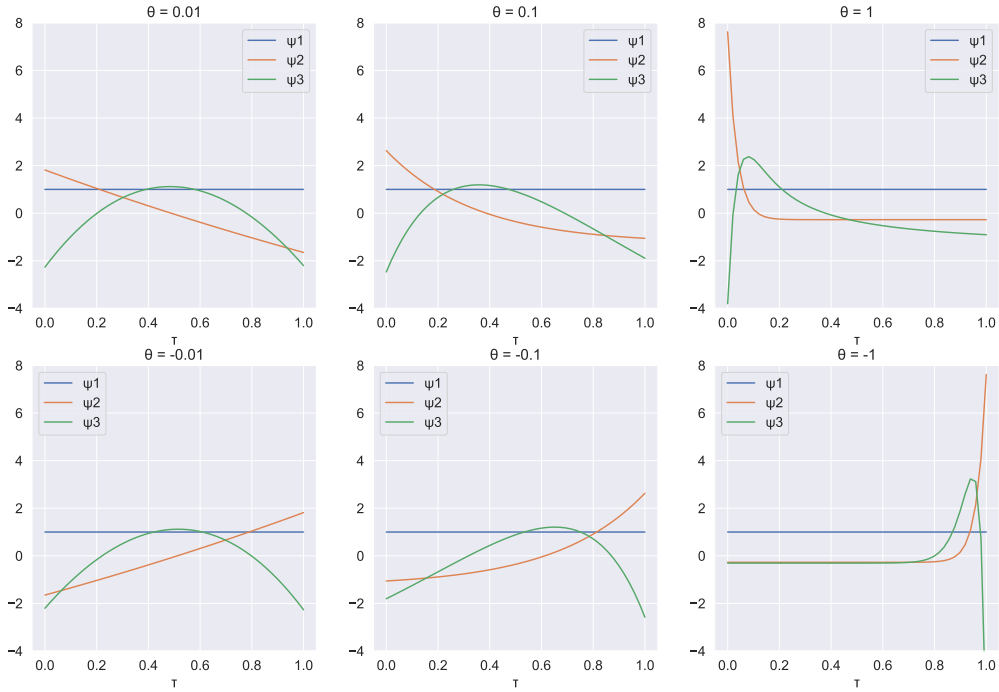


Figure 6: Orthonormal basis  $(\psi_{0k})_{k=1}^3$ .

For the closed-form expressions of the orthonormal basis  $(\psi_{0k})_{k=1}^3$ , refer to **Proof of Theorem 1**.

Letting  $\theta$  vary from a reasonable range, we observe from Figure 6 that  $\psi_{01}$  is always the level,  $\psi_{02}$  the slope, and  $\psi_{03}$  the curvature. Furthermore, with an increase in positive  $\theta$  increases, the slope and the curvature change more drastically at short-maturity bonds; a decrease in negative  $\theta$  pushes the changes of the slope and curvature towards long-term yields. Hence, just like the coefficients  $(\beta_k)_{k=0}^2$  in Eq. (6), the coordinates in the new basis  $(\psi_{0k})_{k=1}^3$  can still be interpreted as the loadings on the level/slope/curvature factors, if they truly are these factors.

If we view  $(\psi_{0k})_{k=1}^3$  as the factors with the most significant loadings among an extended orthonormal set  $(\psi_{0k})_{k=1}^\infty$ , we now proceed to test if  $(\psi_{0k})_{k=1}^\infty$  is equivalent to the actual eigenfunctions  $(\psi_k)_{k=1}^\infty$  up to permutations and changes of sign, i.e., whether the orthonor-

mal basis underlying the Nelson-Siegel model is well-specified to match the actual principal component basis of the covariance kernel  $G$ .

### 3.2 Covariance Estimation

We discretize  $x$  and  $x'$  on an  $N \times N$  grid and estimate a rank- $N$  approximation of the bi-infinite covariance matrix in Eq. (4). The entries of the low-rank sample covariance matrix are shown in Figure 7 for the entire data. The positive entries demonstrate the strong cross-sectional co-movements of yield curves over time. Such co-movements are much stronger on short-term bond yields as concentrated at the upper-left block of Figure 7, which apparently have higher liquidity and respond to the market more effectively than long-term bond yields.

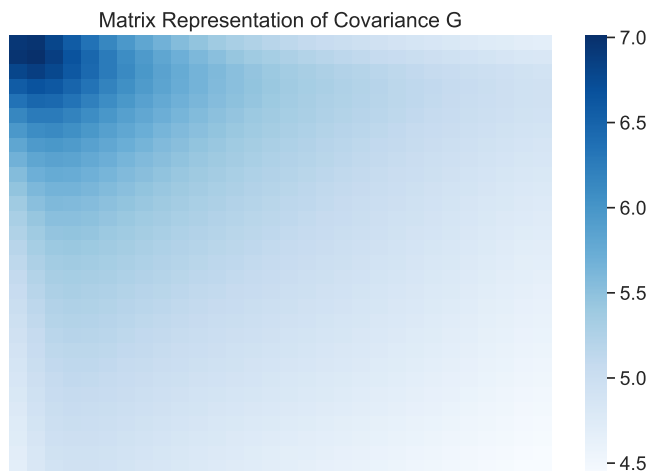


Figure 7:  $\hat{G}$  as a low-rank sample covariance matrix on the entire data ( $N = 30$ ).

However, such a statement is only true when there are no significant frictions in the market. Notice the estimates  $\hat{G}$  are heterogeneous in different years shown in Figure 8. Unlike Hu, Pan and Wang (2013)'s noise measure of liquidity and arbitrage capital that equally weighed the pricing errors of bond yields with different maturities, we argue that the cross-sectional difference in covariance is also indicative for different sources of liquidity. In 1986, for example, the short-term covariation and long-term covariation were both high, while

the covariance between short-term yields and long-term ones stayed low, which indicates that the frictions that drove the illiquid yields might have some components uncorrelated with everyday frictions that mainly impacted the short-term yields, and further gave insights on the 1987 market crash. For another instance, a different but unique covariance structure was observed in both 1992 and 2008, representing the strong and correlated co-movements on both short-term and long-term yields, which could be impacted by factors from the external financial market which tilted the yield curves at their most extreme values, such as the exchange rate risk exposure in the 1992 UK currency crisis and the overall exposure to the global financial crisis in 2008.

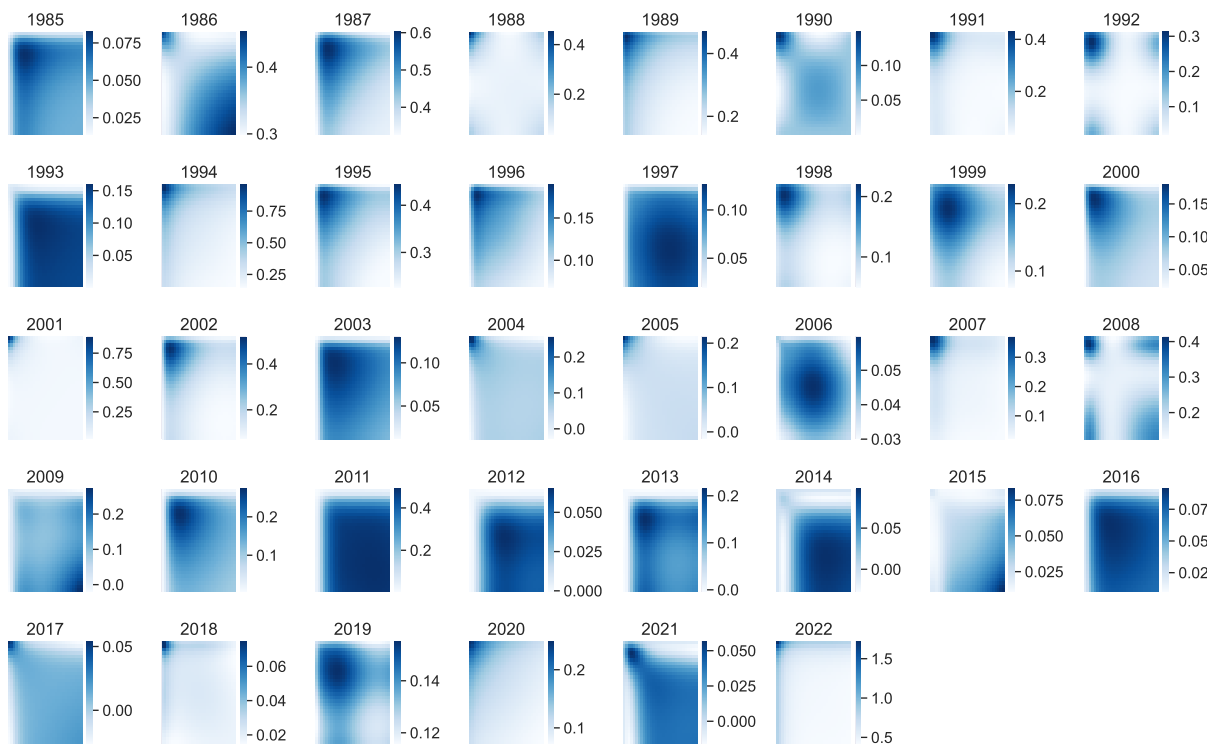


Figure 8: Implied  $\hat{G}$  each year ( $N = 30$ ).

To show the interpretations above are robust with respect to the choice of B-spline subspace and the number of uniform knots  $N$ , so that the projection in Eq. (2) is not overfitting the yield curves, we demonstrate highly similar patterns revealed by Figure 16 using linear B-spline basis and by Figure 18 where  $N = 20$ . This also justifies the robustness

of the estimation of covariance function  $G$ .

### 3.3 Interpreting Functional Principal Components

Based on the covariance estimate  $\hat{G}$ , we first straightforwardly implement FPCA, the results given in Figure 9. The shapes of the first three functional principal components and their explained variance are almost identical to the PCA results in Figure 2.

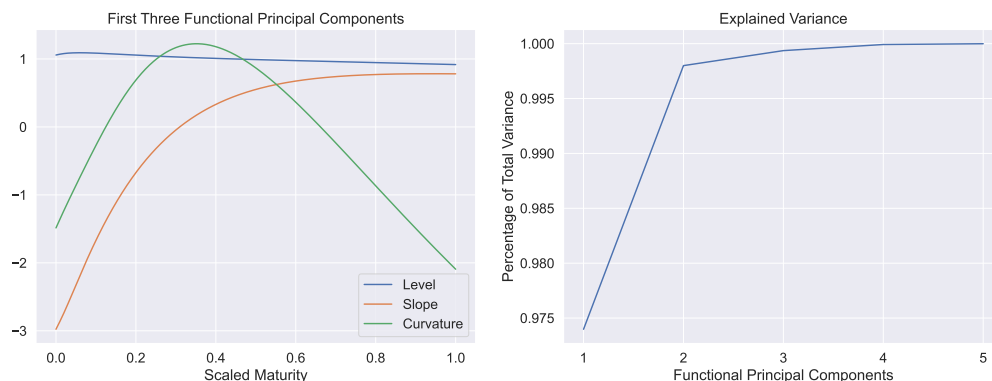


Figure 9: First three functional principal components of the entire dataset and explained variance ratios.

To better illustrate the effects of the obtained functional principal components, we add and subtract the components to the mean function  $\hat{m}$ . We can then observe that the first component (FPC1) shows the parallel shift in the mean  $\hat{m}$ , the second component (FPC2) changes the slope of yield curves by tilting around one knot, the third (FPC3) embeds rich curvature by tilting the yield curve around two fixed knots, FPC4 tilts around 3 points, and so on so forth. Thus, similar interpretations on the level, slope, and curvature to PCA could be given to the functional principal components. Figure 10 offers an intuition of how the flexibility of yield curves can be traced back by their functional principal components. Formally, such intuition is a natural result of the following theorem.

**Theorem 2.** *If the data-generating process with identically distributed (can be dependent)*

zero-mean noise  $\epsilon$  is

$$y(\tau) = \beta_0 + \beta_1 \frac{1 - e^{-\theta_1 \tau}}{\theta_1 \tau} + \beta_2 \left( \frac{1 - e^{-\theta_1 \tau}}{\theta_1 \tau} - e^{-\theta_1 \tau} \right) + \beta_3 \left( \frac{1 - e^{-\theta_2 \tau}}{\theta_2 \tau} - e^{-\theta_2 \tau} \right) + \epsilon, \quad (8)$$

then the number of zeros of the  $k$ -th functional principal component  $|Ker(\psi_k)| \xrightarrow{P} k - 1$ .<sup>6</sup>

Eq. (8) is also the Svensson (1994) specification of yield curves on all maturities, also used in our data after 1980<sup>7</sup> (Gürkaynak, Sack and Wright, 2007) and widely accepted as smoothed yields on hypothetical Treasury securities<sup>8</sup>. Regarding the parameters,  $\theta_i = \frac{1}{\tau_i}$  for  $i = 1, 2$ , and  $(\beta_k)_{k=0}^3$  are the same as the Svensson model.

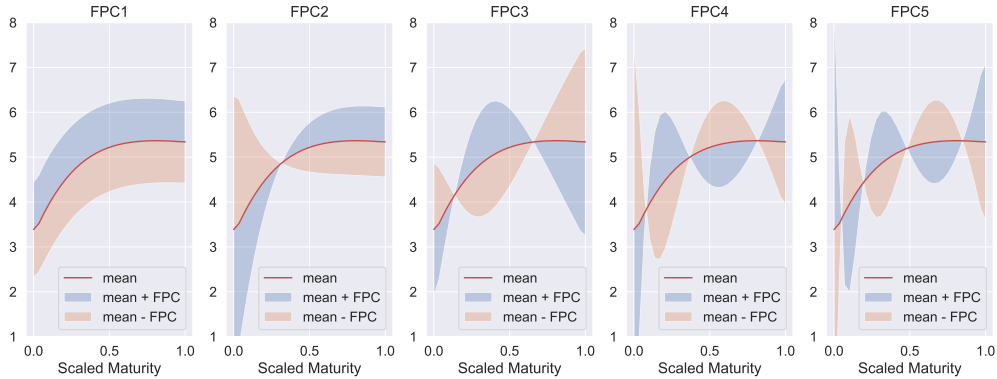


Figure 10: Effects of the functional principal components: blue shades represent the effects of positive shocks in the principal component, and orange shades represent those of negative shocks.

**Theorem 2** also implies that if  $|Ker(\psi_k)|$  deviates a lot from  $k - 1$ , either the regularity conditions imposed on  $\epsilon$  fail to be satisfied, or the sample size is not large enough, or the data-generating process is misspecified. We argue that the former two scenarios are explicitly testable, both involving tests (whether asymptotic or not) on the distribution of  $\epsilon$ . So it would be possible that the model is misspecified after eliminating the former two scenarios.

<sup>6</sup>Here we loosely use  $Ker(f)$  to represent the set of zeros of a function  $f$ . It is not a subspace.

<sup>7</sup>Prior to 1980, the Nelson-Siegel model with fewer parameters was used to fit the yield curve, as there were not enough Treasury securities to fit the Svensson model, which has six parameters.

<sup>8</sup>Refer to the nominal yield curve (<https://www.federalreserve.gov/data/nominal-yield-curve.htm>).

For instance, it might not be appropriate to name the corresponding functional principal components in Figure 11 according to level, slope, and curvature anymore, and the fact that  $|Ker(\psi_k)| \neq k - 1$  for  $k = 2, 3$  is evidence in favor of model misspecification.

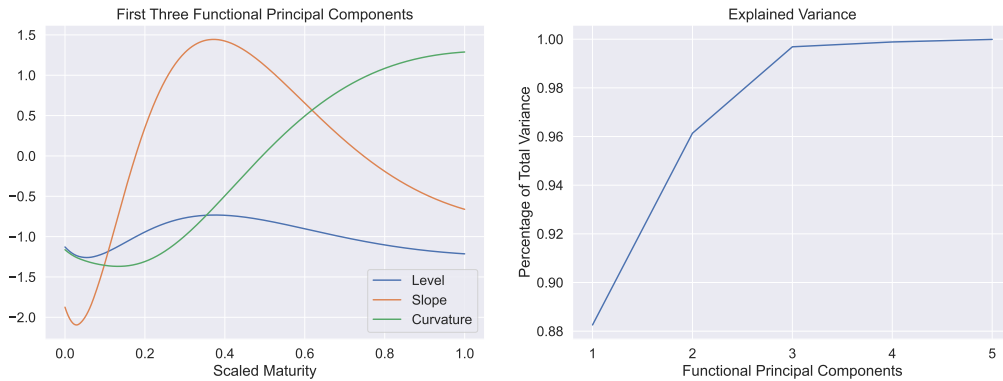


Figure 11: First three functional principal components in 2008 and explained variance ratios.

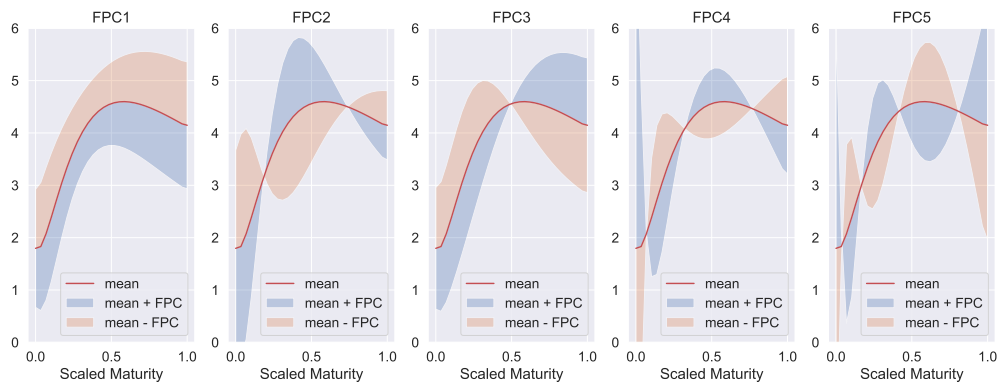


Figure 12: Effects of the functional principal components in 2008:  $|Ker(\psi_2)| = 2$  and  $|Ker(\psi_3)| = 1$ .

### 3.4 Test Statistic and $p$ -value

We now formally compute the test statistic  $\hat{S}_n$  and simulate  $\bar{S}_n$ , the estimated asymptotic distribution of the test statistic under  $H_0$ , in the full sample. The hyper-parameter  $\kappa_n = 3$ , since the eigenvalues  $\lambda_k$  ( $k > 3$ ) are negligible under  $H_0$ , i.e.,  $(\psi_{0k})_{k=1}^3$  given in **Theorem 1** already explains most variation in the yield curves.

Comparing Figure 13 and Figure 1, we see the score  $\zeta_{i1}$  on the first proposed eigenfunction  $\psi_{01}$  captures the macroscopic variation in yield curves of all maturities, as a natural result of the definition of functional principal component analysis.

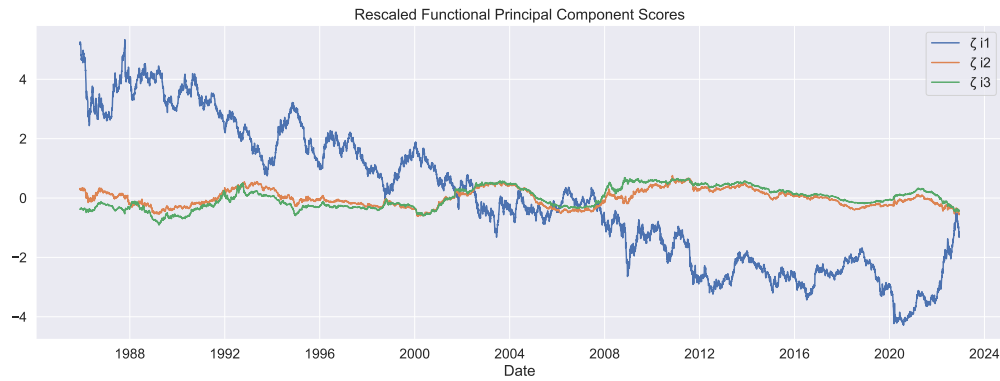


Figure 13: Rescaled functional principal component scores for  $(\psi_{0k})_{k=1}^3$ .

Directly applying the test in Song, Yang and Zhang (2022) for a set of possible parameters  $\theta \in \{\pm 0.001, \pm 0.01, \pm 0.1, 0.2, 0.5, 1\}$  for the Nelson-Siegel orthonormal basis,  $H_0$  is rejected both on the entire sample and on almost each yearly data with  $p \ll 0.05$  shown in Figure 14. This means that the Nelson-Siegel basis in general cannot be interpreted as the principal components, and there is strong evidence in the model being misspecified.

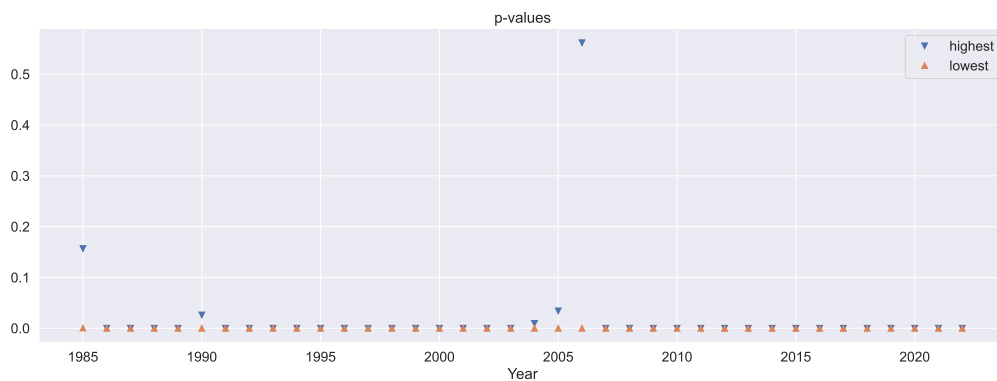


Figure 14: In the Song-Yang-Zhang test, the highest and lowest  $p$ -values attained for different parameter  $\theta$  in each year.

To further gain some insights on how confident we are when regarding the Nelson-Siegel

orthonormal basis as the principal components, we loosen the above test statistic in **Theorem 3**.

**Theorem 3.** *Modify the Song-Yang-Zhang test statistic in Eq. (3) to*

$$\hat{S}_n = n \sum_{1 \leq k \neq k' \leq \kappa_n} \hat{Z}_{kk'}^2,$$

and the asymptotic distribution in Eq. (5) to

$$\bar{S}_n = \sum_{1 \leq k \neq k' \leq \kappa_n} \hat{\lambda}_k \hat{\lambda}_{k'} \chi_{kk'}^2(1) + \sum_{k=1}^{\kappa_n} \hat{\lambda}_k^2 \left( \frac{1}{n} \sum_{i=1}^n \|\hat{\xi}_i^2\|^2 - 1 \right) \chi_{kk}^2(1).$$

Then the test is still consistent at asymptotic level of significance  $\alpha$ , i.e., under  $H_0$ ,

$$P(\hat{S}_n > \hat{Q}_{1-\alpha}) \rightarrow \alpha;$$

and under  $H_1$ ,

$$P(\hat{S}_n > \hat{Q}_{1-\alpha}) \rightarrow 1,$$

where  $\hat{Q}_{1-\alpha}$  is the  $100(1 - \alpha)$ -th percentile of  $\bar{S}_n$ .

Now we proceed to conduct the hypothesis test in **Theorem 3** on the full sample. The  $p$ -values reported in Table 1 suggest that the Nelson-Siegel basis  $(\psi_{0k})_{k=1}^3$  is not highly sensitive enough to the parameter  $\theta$  to influence the test conclusion within a reasonable range (e.g.,  $|\theta| \in [0.01, 0.2]$ ). Hence there is probably rich flexibility embedded by  $\theta$  in the Nelson-Siegel model.

$\theta$	$p$ -values
-0.1	0.1944
-0.01	0.1946
-0.001	0.0932
0.001	0.0515
0.01	0.1925
0.1	0.1724
0.2	0.1506
0.5	0.0744
1	0.0169*

Table 1:  $p$ -values on full sample for different values of  $\theta$ .

However, the heterogeneity of the test results each year is demonstrated by Figure 15. We notice that when the highest  $p$ -values attained are low (so that there is evidence in favor of  $H_1$ , and the level-slope-curvature argument is suspicious), there was a recession or some influential adjustments on the interest rate policies. In 2014, for instance, the Federal Reserve ceased its expansion in holding longer-term securities through open market purchases, originally aiming at putting downward pressure on longer-term interest rates and supporting economic activities through making more accommodating financial conditions. 2007 marked that the Federal Reserve cut the target on short-term interest rate by half of a percentage point. The recession and RTC in 1991, and the UK currency crisis in 1992 causes explainable deviations to the reference model as well. These are all possible shocks that lead to interest rate model deviating from the level-slope-curvature component structure.

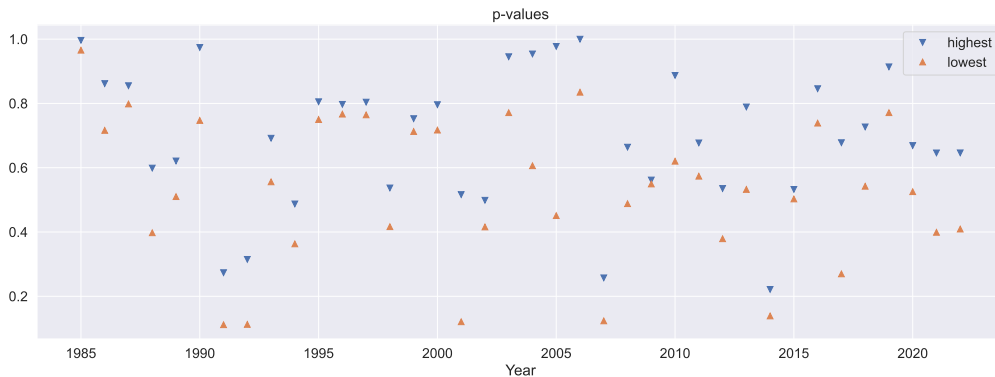


Figure 15: The highest and lowest  $p$ -values attained for different parameter  $\theta$  in each year based on the test in **Theorem 3**.

## 4 Conclusions

This paper investigates the model misspecification of interest rate term structure using functional principal component analysis. We first show by orthonormalization in the function space that the Nelson-Siegel model, as a standard reference model, can be interpreted as a three-factor interest rate term structure involving the level, the slope, and the curvature. This justifies the presence of the Nelson-Siegel orthonormal basis in the null hypothesis to test whether the actual data-driven principal components coincide with the level/slope/curvature factors, i.e., whether (and when) the three-factor model is misspecified.

Two notions have been used to determine whether two bases are the same. The stricter one in Section 3.3 offers a non-rigorous way to test whether the functional principal components match the level, the slope, and the curvature in the exact order. We conclude from the entire sample that the components appear in the desired order, which is not the case for specific individual years. For instance, in 2008, a curvature factor potentially explained more variance than a slope factor. The same conclusion is drawn based on the other less strict notion in Section 3.4, where permutations and sign changes in the basis are accepted. To sum up, this paper characterizes the heterogeneity of misspecification in the interest rate term structure when rare events or relevant shocks in policies occur, even if the model is

accepted overall.

Future research could generalize the proposed methodology to test the reference models other than the Nelson-Siegel model, which lacks financial intuition compared to other affine models such as Vasicek (1977), and to include calibration from the actual market data in bond yields rather than merely hypothetical securities.

## References

- Anderson, Evan, Lars Peter Hansen, and Thomas Sargent.** 2000. “Robustness, detection and the price of risk.” mimeo.
- Ang, Andrew, Robert J Hodrick, Yuhang Xing, and Xiaoyan Zhang.** 2006. “The cross-section of volatility and expected returns.” *The journal of finance*, 61(1): 259–299.
- Bodenham, Dean A, and Niall M Adams.** 2016. “A comparison of efficient approximations for a weighted sum of chi-squared random variables.” *Statistics and Computing*, 26(4): 917–928.
- Brenner, Robin J, Richard H Harjes, and Kenneth F Kroner.** 1996. “Another look at models of the short-term interest rate.” *Journal of financial and quantitative analysis*, 31(1): 85–107.
- Chapman, David A, and Neil D Pearson.** 2001. “Recent advances in estimating term-structure models.” *Financial Analysts Journal*, 57(4): 77–95.
- Christensen, Jens HE, Francis X Diebold, and Glenn D Rudebusch.** 2011. “The affine arbitrage-free class of Nelson–Siegel term structure models.” *Journal of Econometrics*, 164(1): 4–20.
- Cont, Rama.** 2005. “Modeling term structure dynamics: an infinite dimensional approach.” *International Journal of theoretical and applied finance*, 8(03): 357–380.
- Davies, Robert B.** 1980. “Algorithm AS 155: The distribution of a linear combination of  $\chi^2$  random variables.” *Applied Statistics*, 323–333.
- Diebold, Francis X, and Canlin Li.** 2006. “Forecasting the term structure of government bond yields.” *Journal of econometrics*, 130(2): 337–364.
- Diebold, Francis X, Canlin Li, and Vivian Z Yue.** 2008. “Global yield curve dynamics and interactions: a dynamic Nelson–Siegel approach.” *Journal of Econometrics*, 146(2): 351–363.
- Elenev, Vadim, Tim Landvoigt, and Stijn Van Nieuwerburgh.** 2022. “Can the COVID bailouts save the economy?” *Economic Policy*, 37(110): 277–330.
- Elenev, Vadim, Tim Landvoigt, Patrick J Shultz, and Stijn Van Nieuwerburgh.** 2021. “Can monetary policy create fiscal capacity?” National Bureau of Economic Research.
- Fama, Eugene F, and James D MacBeth.** 1973. “Risk, return, and equilibrium: Empirical tests.” *Journal of political economy*, 81(3): 607–636.
- Fisher, Mark, Douglas W Nychka, and David Zervos.** 1995. “Fitting the term structure of interest rates with smoothing splines.”
- Giannoni, Marc P.** 2002. “Does model uncertainty justify caution? Robust optimal mon-

- etary policy in a forward-looking model.” *Macroeconomic Dynamics*, 6(1): 111–144.
- Gürkaynak, Refet S, Brian Sack, and Jonathan H Wright.** 2007. “The US Treasury yield curve: 1961 to the present.” *Journal of monetary Economics*, 54(8): 2291–2304.
- Hall, Peter, Hans-Georg Müller, and Jane-Ling Wang.** 2006. “Properties of principal component methods for functional and longitudinal data analysis.” *The annals of statistics*, 34(3): 1493–1517.
- Hansen, Lars Peter, and Thomas J Sargent.** 2001*a*. “Acknowledging misspecification in macroeconomic theory.” *Review of Economic Dynamics*, 4(3): 519–535.
- Hansen, LarsPeter, and Thomas J Sargent.** 2001*b*. “Robust control and model uncertainty.” *American Economic Review*, 91(2): 60–66.
- Hansen, Lars Peter, and Thomas J Sargent.** 2010. “Wanting robustness in macroeconomics.” In *Handbook of monetary economics*. Vol. 3, 1097–1157. Elsevier.
- Hansen, Lars Peter, Thomas J Sargent, and Thomas D Tallarini Jr.** 1999. “Robust permanent income and pricing.” *Review of Economic studies*, 873–907.
- Hou, Kaiwen, and Bin Li.** 2021. “A New Proof of Sturm’s Theorem via Matrix Theory.” *arXiv preprint arXiv:2110.15364*.
- Hou, Kaiwen, and Guillaume Rabusseau.** 2022. “Spectral Regularization: an Inductive Bias for Sequence Modeling.” *arXiv preprint arXiv:2211.02255*.
- Hu, Grace Xing, Jun Pan, and Jiang Wang.** 2013. “Noise as information for illiquidity.” *The Journal of Finance*, 68(6): 2341–2382.
- Johannes, Michael.** 2004. “The statistical and economic role of jumps in continuous-time interest rate models.” *The Journal of Finance*, 59(1): 227–260.
- Jouzani, Neda Mohammadi, and Victor M Panaretos.** 2021. “Functional Data Analysis with Rough Sampled Paths?” *arXiv preprint arXiv:2105.12035*.
- Kasa, Kenneth.** 2002. “Model uncertainty, robust policies, and the value of commitment.” *Macroeconomic Dynamics*, 6(1): 145–166.
- Koijen, Ralph SJ, Hanno Lustig, and Stijn Van Nieuwerburgh.** 2017. “The cross-section and time series of stock and bond returns.” *Journal of Monetary Economics*, 88: 50–69.
- Kosambi, DD.** 2016. “Statistics in function space.” In *DD Kosambi*. 115–123. Springer.
- Krishnamurthy, Arvind, and Annette Vissing-Jorgensen.** 2011. “The effects of quantitative easing on interest rates: channels and implications for policy.” National Bureau of Economic Research.
- Kusuoka, Shigeo.** 2000. “Term structure and SPDE.” In *Advances in mathematical economics*. 67–85. Springer.
- Litterman, Robert, and Jose Scheinkman.** 1991. “Common factors affecting bond re-

- turns.” *Journal of fixed income*, 1(1): 54–61.
- Liu, Yu, Hao Wang, and Lihong Zhang.** 2018. “Return Ambiguity, Portfolio Choice, and Asset Pricing.” *Portfolio Choice, and Asset Pricing (November 11, 2018)*.
- Liu, Yu, Hao Wang, Tan Wang, and Lihong Zhang.** 2022. “Volatility Ambiguity, Portfolio Decisions, and Equilibrium Asset Pricing.” *Portfolio Decisions, and Equilibrium Asset Pricing (August 25, 2022)*.
- Li, Yehua, and Tailen Hsing.** 2010. “Uniform convergence rates for nonparametric regression and principal component analysis in functional/longitudinal data.” *The Annals of Statistics*, 38(6): 3321–3351.
- Lord, Roger, and Antoon Pelsser.** 2007. “Level–slope–curvature–fact or artefact?” *Applied Mathematical Finance*, 14(2): 105–130.
- Maenhout, Pascal J.** 2004. “Robust portfolio rules and asset pricing.” *Review of financial studies*, 17(4): 951–983.
- McCulloch, J Huston.** 1975. “The tax-adjusted yield curve.” *The Journal of Finance*, 30(3): 811–830.
- Nelson, Charles R, and Andrew F Siegel.** 1987. “Parsimonious modeling of yield curves.” *Journal of business*, 473–489.
- Onatski, Alexei, and James H Stock.** 2002. “Robust monetary policy under model uncertainty in a small model of the US economy.” *Macroeconomic Dynamics*, 6(1): 85–110.
- Piazzesi, Monika.** 2010. “Affine term structure models.” In *Handbook of financial econometrics: Tools and Techniques*. 691–766. Elsevier.
- Song, Zening, Lijian Yang, and Yuanyuan Zhang.** 2022. “Hypotheses Testing of Functional Principal Components.”
- Staniswalis, Joan G, and J Jack Lee.** 1998. “Nonparametric regression analysis of longitudinal data.” *Journal of the American Statistical Association*, 93(444): 1403–1418.
- Svensson, Lars EO.** 1994. “Estimating and interpreting forward interest rates: Sweden 1992-1994.”
- Vasicek, Oldrich.** 1977. “An equilibrium characterization of the term structure.” *Journal of financial economics*, 5(2): 177–188.
- Woodford, Michael.** 2010. “Robustly optimal monetary policy with near-rational expectations.” *American Economic Review*, 100(1): 274–303.
- Woodford, Michael.** 2012. “Methods of policy accommodation at the interest-rate lower bound.”
- Yao, Fang, Hans-Georg Müller, and Jane-Ling Wang.** 2005a. “Functional data analysis for sparse longitudinal data.” *Journal of the American statistical association*,

100(470): 577–590.

**Yao, Fang, Hans-Georg Müller, and Jane-Ling Wang.** 2005*b*. “Functional linear regression analysis for longitudinal data.” *The Annals of Statistics*, 33(6): 2873–2903.

**Zhang, Lihong, Bingqian Cheng, and Hao Wang.** 2022. “Optimal Investment for Insurers with Correlation Ambiguity.” *Available at SSRN 4025188*.

## Appendix A. Proofs

**Sketchy Proof of Theorem 1.** *Proof.* Consider the following rescaling of  $\tau$

$$\tilde{\tau} = \frac{\tau - \underline{\tau}}{\bar{\tau} - \underline{\tau}} \in [0, 1].$$

Then Eq. (6) becomes

$$\hat{y}(\tilde{\tau} \mid \Theta) = \sum_{k=1}^3 \alpha_k \Psi_{0k}(\tilde{\tau}) \in L^2([0, 1], d\xi),$$

where the basis functions

$$\begin{aligned} \Psi_{01}(\tilde{\tau}) &= 1, \\ \Psi_{02}(\tilde{\tau}) &= e^{-\theta\tau} = \exp\{-\theta[(\bar{\tau} - \underline{\tau})\tilde{\tau} + \underline{\tau}]\} = \exp\{-(A\tilde{\tau} + B)\}, \\ \Psi_{03}(\tilde{\tau}) &= \frac{1 - e^{-\theta\tau}}{\theta\tau} = \frac{1 - \exp\{-\theta[(\bar{\tau} - \underline{\tau})\tilde{\tau} + \underline{\tau}]\}}{\theta[(\bar{\tau} - \underline{\tau})\tilde{\tau} + \underline{\tau}]} = \frac{1 - \exp\{-(A\tilde{\tau} + B)\}}{A\tilde{\tau} + B}, \end{aligned}$$

with

$$\begin{aligned} A &= \theta(\bar{\tau} - \underline{\tau}), \\ B &= \theta\underline{\tau}, \end{aligned}$$

and the coordinates

$$(\alpha_1, \alpha_2, \alpha_3)' = (\beta_0, -\beta_2, \beta_1 + \beta_2)'.$$

Now we follow the Gram–Schmidt process to obtain an orthonormal basis  $(\psi_{0k})_{k=1}^3$  for the subspace  $Span(\Psi_{0k})_{k=1}^3$ . Start with  $\psi_{01} = \Psi_{01} = 1$ , which satisfies  $\|\psi_{01}\|^2 = \int_0^1 d\xi = 1$ . Consider the projection of  $\Psi_{02}$  onto  $\psi_{01}$

$$\mathcal{P}_{\psi_{01}} \Psi_{02} = \frac{\langle \psi_{01}, \Psi_{02} \rangle}{\langle \psi_{01}, \psi_{01} \rangle} \psi_{01} = \int_0^1 \exp\{-(A\xi + B)\} d\xi = \frac{e^{-B} - e^{-A-B}}{A} =: D.$$

Then

$$\tilde{\psi}_{02} = \Psi_{02} - \mathcal{P}_{\psi_{01}} \Psi_{02} = \exp \{-(A\tilde{\tau} + B)\} - D,$$

with

$$\begin{aligned} \|\tilde{\psi}_{02}\|^2 &= \langle \tilde{\psi}_{02}, \tilde{\psi}_{02} \rangle \\ &= \frac{1}{2A}(e^{-2B} - e^{-2(A+B)}) - \frac{2D}{A}(e^{-B} - e^{-A-B}) + D^2 \\ &= \frac{1}{2A}(e^{-2B} - e^{-2(A+B)}) - D^2. \end{aligned}$$

Thus,

$$\psi_{02} = \frac{\tilde{\psi}_{02}}{\|\tilde{\psi}_{02}\|}.$$

The projection of  $\Psi_{03}$  onto  $\psi_{01}$  is

$$\begin{aligned} \mathcal{P}_{\psi_{01}} \Psi_{03} &= \frac{\langle \psi_{01}, \Psi_{03} \rangle}{\langle \psi_{01}, \psi_{01} \rangle} \psi_{01} \\ &= \int_0^1 \frac{1 - \exp \{-(A\xi + B)\}}{A\xi + B} d\xi \\ &= \frac{\log |A + B| - \log |B| - Ei(-A - B) + Ei(-B)}{A} \\ &= \frac{\log |A + B| - \log |B|}{A} - \frac{Ei(-A - B) - Ei(-B)}{A} := F - H, \end{aligned}$$

where  $Ei$  is the exponential integral. The projection of  $\Psi_{03}$  onto  $\tilde{\psi}_{02}$  is

$$\mathcal{P}_{\tilde{\psi}_{02}} \Psi_{03} = \frac{\langle \tilde{\psi}_{02}, \Psi_{03} \rangle}{\langle \tilde{\psi}_{02}, \tilde{\psi}_{02} \rangle} \tilde{\psi}_{02} = \frac{\tilde{\psi}_{02}}{\|\tilde{\psi}_{02}\|^2} \langle \tilde{\psi}_{02}, \Psi_{03} \rangle,$$

where

$$\begin{aligned}
\langle \tilde{\psi}_{02}, \Psi_{03} \rangle &= \int_0^1 (\exp \{-(A\xi + B)\} - D) \frac{1 - \exp \{-(A\xi + B)\}}{A\xi + B} d\xi \\
&= \int_0^1 \frac{\exp \{-(A\xi + B)\} - \exp \{-2(A\xi + B)\}}{A\xi + B} d\xi - D \int_0^1 \frac{1 - \exp \{-(A\xi + B)\}}{A\xi + B} d\xi \\
&= \frac{Ei(-A - B) - Ei(-B) - Ei(-2A - 2B) + Ei(-2B)}{A} - D(F - H) \\
&= H - \frac{Ei(-2A - 2B) - Ei(-2B)}{A} - D(F - H) \\
&= (D + 1)H - DF - \frac{Ei(-2A - 2B) - Ei(-2B)}{A} =: J.
\end{aligned}$$

Then

$$\begin{aligned}
\tilde{\psi}_{03} &= \Psi_{03} - \mathcal{P}_{\psi_{01}} \Psi_{03} - \mathcal{P}_{\tilde{\psi}_{02}} \Psi_{03} \\
&= \frac{1 - \exp \{-(A\tilde{\tau} + B)\}}{A\tilde{\tau} + B} - F + H - \frac{J\tilde{\psi}_{02}}{\|\tilde{\psi}_{02}\|^2} \\
&= \frac{1 - \exp \{-(A\tilde{\tau} + B)\}}{A\tilde{\tau} + B} + K \exp \{-(A\tilde{\tau} + B)\} + L,
\end{aligned}$$

where

$$\begin{aligned}
K &:= -\frac{J}{\|\tilde{\psi}_{02}\|^2}, \\
L &:= -F + H + \frac{JD}{\|\tilde{\psi}_{02}\|^2}.
\end{aligned}$$

Finally,

$$\begin{aligned}
\|\tilde{\psi}_{03}\|^2 &= \langle \tilde{\psi}_{03}, \tilde{\psi}_{03} \rangle \\
&= \int_0^1 \left( \frac{1 - \exp\{-(A\xi + B)\}}{A\xi + B} \right)^2 d\xi + K^2 \int_0^1 \exp\{-2(A\xi + B)\} d\xi + L^2 \\
&\quad + 2K \int_0^1 \frac{\exp\{-(A\xi + B)\} - \exp\{-2(A\xi + B)\}}{A\xi + B} d\xi \\
&\quad + 2L \int_0^1 \frac{1 - \exp\{-(A\xi + B)\}}{A\xi + B} d\xi \\
&\quad + 2KL \int_0^1 \exp\{-(A\xi + B)\} d\xi \\
&= \frac{1}{B(A+B)} + \frac{2e^{-A-B}}{A(A+B)} + \frac{2Ei(-A-B)}{A} - \frac{2e^{-B}}{AB} - \frac{2Ei(-B)}{A} - \frac{e^{-2A-2B}}{A(A+B)} \\
&\quad - \frac{2Ei(-2A-2B)}{A} + \frac{e^{-2B}}{AB} + \frac{2Ei(-2B)}{A} + K^2 \frac{e^{-2B} - e^{-2(A+B)}}{2A} + L^2 \\
&\quad + 2K \left( H - \frac{Ei(-2A-2B) - Ei(-2B)}{A} \right) + 2L(F - H) + 2KLD,
\end{aligned}$$

and

$$\psi_{03} = \frac{\tilde{\psi}_{03}}{\|\tilde{\psi}_{03}\|}.$$

So far, we have recovered an orthonormal basis  $(\psi_{0k})_{k=1}^3$ .

□

**Sketchy Proof of Theorem 2.** *Proof.* For notational simplicity, write

$$\begin{aligned}
\Psi_{02}^\theta(\tau) &= e^{-\theta\tau}, \\
\Psi_{03}^\theta(\tau) &= \frac{1 - e^{-\theta\tau}}{\theta\tau},
\end{aligned}$$

for  $\theta \in \{\theta_1, \theta_2\}$ . Then Eq. (8) becomes

$$\begin{aligned} y &= \beta_0 + \beta_1 \Psi_{03}^{\theta_1} + \beta_2 (\Psi_{03}^{\theta_1} - \Psi_{02}^{\theta_1}) + \beta_3 (\Psi_{03}^{\theta_2} - \Psi_{02}^{\theta_2}) + \epsilon \\ &= \beta_0 + (\beta_1 + \beta_2) \Psi_{03}^{\theta_1} - \beta_2 \Psi_{02}^{\theta_1} + \beta_3 \Psi_{03}^{\theta_2} - \beta_3 \Psi_{02}^{\theta_2} + \epsilon. \end{aligned} \quad (9)$$

Compute the first-order derivatives

$$\begin{aligned} \frac{\partial}{\partial \tau} \Psi_{03}^{\theta} &= -\theta \left( \frac{1 - e^{-\theta\tau}}{\theta^2 \tau^2} - \frac{e^{-\theta\tau}}{\theta\tau} \right) \\ &= -\frac{1}{\tau} \left( \frac{1 - e^{-\theta\tau}}{\theta\tau} - e^{-\theta\tau} \right) \\ &= -\frac{1}{\tau} (\Psi_{03}^{\theta} - \Psi_{02}^{\theta}) \end{aligned}$$

and

$$\frac{\partial}{\partial \tau} \Psi_{02}^{\theta} = -\theta \Psi_{02}^{\theta}.$$

The second-order derivatives are hence

$$\begin{aligned} \frac{\partial^2}{\partial \tau^2} \Psi_{03}^{\theta} &= -\frac{1}{\tau^2} \left( \tau \frac{\partial}{\partial \tau} \Psi_{03}^{\theta} - \Psi_{03}^{\theta} - \tau \frac{\partial}{\partial \tau} \Psi_{02}^{\theta} + \Psi_{02}^{\theta} \right) \\ &= -\frac{1}{\tau^2} (\Psi_{02}^{\theta} - 2\Psi_{03}^{\theta} + (\theta\tau + 1)\Psi_{02}^{\theta}) \\ &= \frac{1}{\tau^2} (2\Psi_{03}^{\theta} - (\theta\tau + 2)\Psi_{02}^{\theta}) \end{aligned}$$

and

$$\frac{\partial^2}{\partial \tau^2} \Psi_{02}^{\theta} = -\theta \frac{\partial}{\partial \tau} \Psi_{02}^{\theta} = \theta^2 \Psi_{02}^{\theta}.$$

Under some regularity conditions on  $\epsilon$ , we can take the derivatives in Eq. (9):

$$\frac{\partial y}{\partial \tau} = -\frac{\beta_1 + \beta_2}{\tau} (\Psi_{03}^{\theta_1} - \Psi_{02}^{\theta_1}) + \beta_2 \theta_1 \Psi_{02}^{\theta_1} - \frac{\beta_3}{\tau} (\Psi_{03}^{\theta_2} - \Psi_{02}^{\theta_2}) + \beta_3 \theta_2 \Psi_{02}^{\theta_2}$$

and

$$\frac{\partial^2 y}{\partial \tau^2} = \frac{\beta_1 + \beta_2}{\tau^2} [2\Psi_{03}^{\theta_1} - (\theta_1\tau + 2)\Psi_{02}^{\theta_1}] - \beta_2\theta_1^2\Psi_{02}^{\theta_1} + \frac{\beta_3}{\tau^2} [2\Psi_{03}^{\theta_2} - (\theta_2\tau + 2)\Psi_{02}^{\theta_2}] - \beta_3\theta_2^2\Psi_{02}^{\theta_2}.$$

Impose the ansatz that there exist

- $p \in C^1[\underline{\tau}, \bar{\tau}]$ ,
- $q \in C^0[\underline{\tau}, \bar{\tau}]$ ,
- $r \in C^0(0, \infty)$  s.t.  $r(\lambda_k) \uparrow \infty$ ,

satisfying

$$p\frac{\partial^2 y}{\partial \tau^2} + p'\frac{\partial y}{\partial \tau} + qy = -ry,$$

or

$$\frac{\partial}{\partial \tau} \left( p \frac{\partial y}{\partial \tau} \right) + qy = -ry. \quad (10)$$

The ansatz could be verified by matching the coefficients. Then Eq. (10) with well-defined boundary conditions constitutes a regular Sturm–Liouville problem.

According to the Sturm–Liouville theory, the  $k$ -th fundamental solution corresponding to the eigenvalue  $\lambda_k$  is the unique eigenfunction  $\psi_k$  with exactly  $k - 1$  zeros in  $(\underline{\tau}, \bar{\tau})$  (in the probability limit under some regularity conditions for  $\epsilon$ ). Thus,

$$|Ker(\psi_k)| \xrightarrow{p} k - 1.$$

A special case of Sturm–Liouville theory when  $\psi_k$ 's are real polynomials is presented in Hou and Li (2021), which also applies for many proposed  $\psi_{0k}$  (e.g., in B-spline basis as the case in this paper, in monomial basis, or even in the orthonormal basis in **Theorem 1** up to the errors of Taylor expansion of the exponential).

□

**Sketchy Proof of Theorem 3.** *Proof.* Let

$$\mathbf{Y}_i = (\zeta_{ik}\zeta_{ik'} - \lambda_k\delta_{kk'})_{k,k'=1}^\infty,$$

where  $\delta$  is the Kronecker delta. According to Song, Yang and Zhang (2022), the Hilbert central limit theorem yields

$$\frac{1}{\sqrt{n}} \sum_{i=1}^n \mathbf{Y}_i \xrightarrow{d} \mathbf{N} \sim \mathcal{N}(\mathbf{0}, \mathbf{C}_\mathbf{Y})$$

with the covariance function

$$\mathbf{C}_\mathbf{Y}(\mathbf{e}_{kk}) = \lambda_k^2 (\mathbb{E}\xi_i^4 - 1) \mathbf{e}_{kk},$$

and

$$\mathbf{C}_\mathbf{Y}(\mathbf{e}_{kk'}) = \lambda_k \lambda_{k'} \mathbf{e}_{kk'}.$$

Hence

$$\frac{\mathbf{N}_{kk}^2}{\lambda_k^2 (\mathbb{E}\xi_i^4 - 1)}, \frac{\mathbf{N}_{kk'}^2}{\lambda_k \lambda_{k'}} \sim \chi^2(1).$$

Then by continuous mapping theorem, the Frobenius norm

$$\begin{aligned} \left\| \frac{1}{\sqrt{n}} \sum_{i=1}^n \mathbf{Y}_i \right\|_F^2 &\xrightarrow{d} \|\mathbf{N}\|_F^2 \\ &= \sum_{1 \leq k \neq k' < \infty} \lambda_k \lambda_{k'} \chi_{kk'}^2(1) + \sum_{k=1}^{\infty} \lambda_k^2 (\mathbb{E}\xi_i^4 - 1) \chi_{kk}^2(1). \end{aligned} \quad (11)$$

Clearly, under  $H_0$ ,

$$n \sum_{1 \leq k, k' < \infty} Z_{kk'}^2 = \left\| \frac{1}{\sqrt{n}} \sum_{i=1}^n \mathbf{Y}_i \right\|_F^2. \quad (12)$$

In the infeasible Gaussian quadratic form in Eq. (11), replace  $\lambda$  and  $\mathbb{E}\xi_i^4$  by their sample estimates and restrict the summation by the finite number  $\kappa_n$ . Similarly, replace the left-

hand side in Eq. (12) by  $\hat{S}_n$ . The rest of the proof follows in a straightforward manner as Song, Yang and Zhang (2022).

□

## Appendix B. Robustness

We demonstrate the robustness of our interpretations of Figure 8 by showing its independence on the choice of  $N$  and  $p$  in Eq. (2) as long as the yield curves are not overfit.

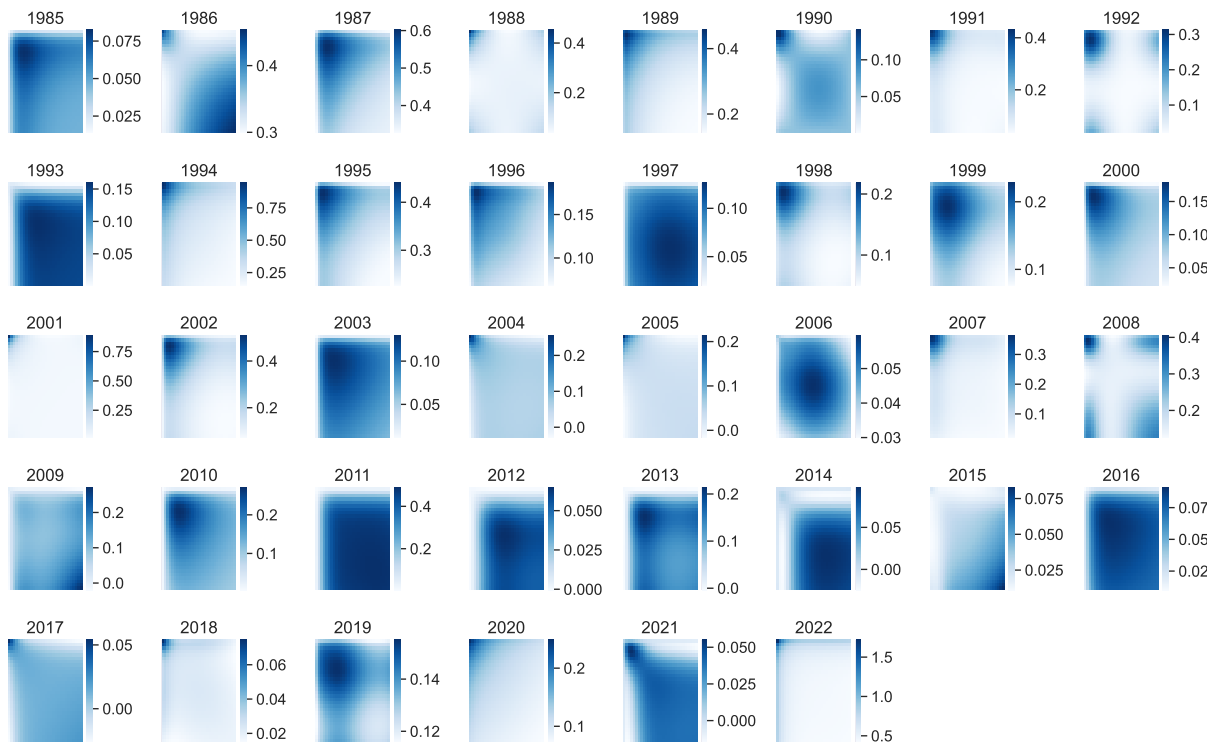


Figure 16: Yearly implied  $\hat{G}$  fitted with linear B-splines and 30 uniform knots.

The functional principal components still exhibit similar properties as in Figure 9.

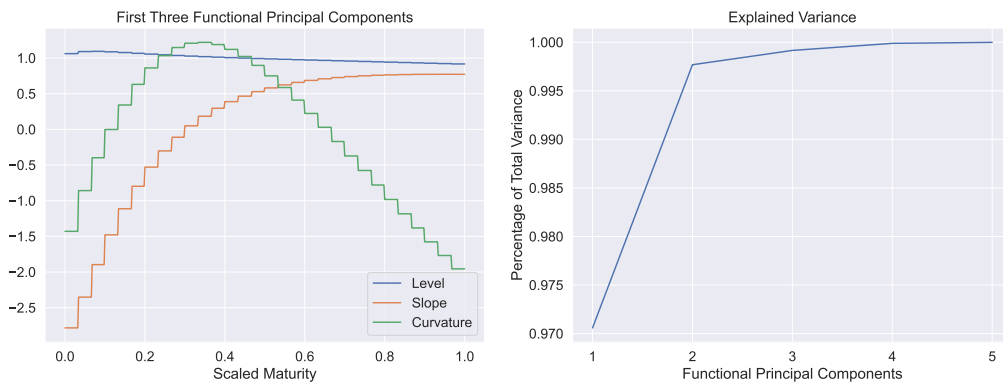


Figure 17: First three functional principal components with  $\hat{G}$  fitted with linear B-splines and 30 uniform knots.

The number of knots is an even minor issue to our results. There is almost no discernible difference in the FPCA results using fewer uniform knots, so we omit the plot here.

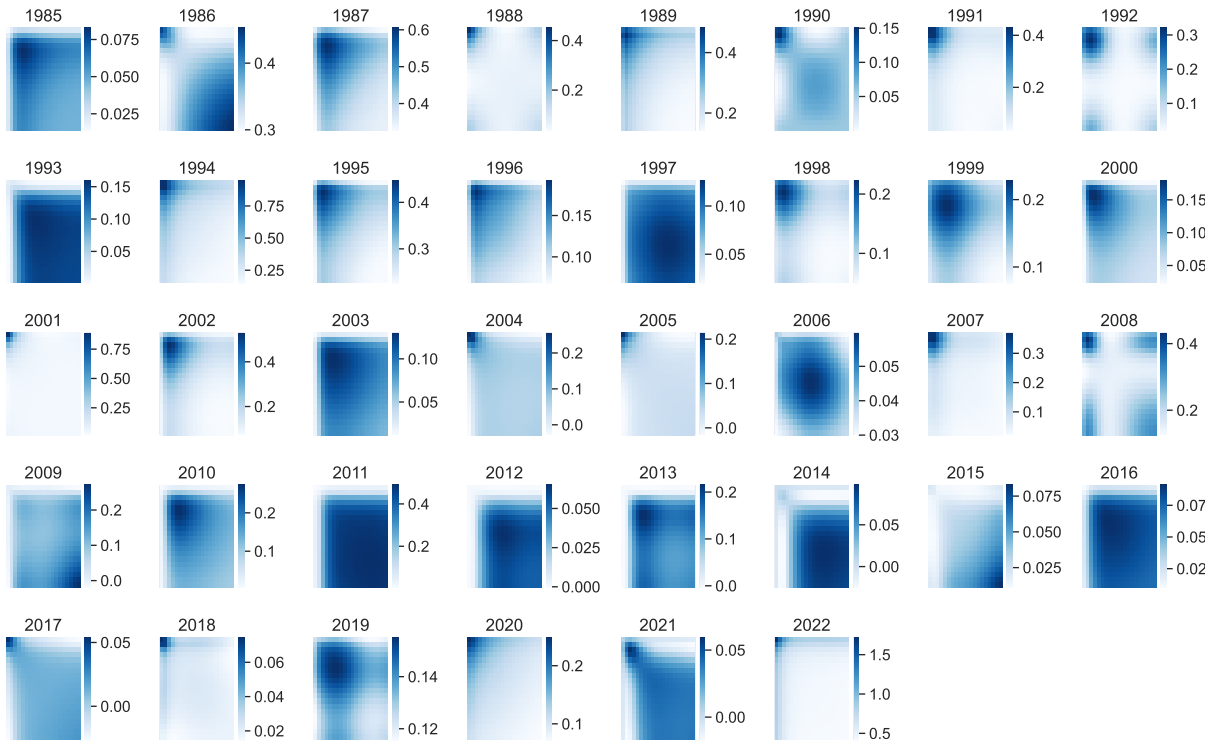


Figure 18: Yearly implied  $\hat{G}$  fitted with cubic B-splines and 20 uniform knots.